DITP 0.5 μM IMAGING LADAR TARGET SPECKLE STATISTICS AND THEIR IMPACT ON DISCRIMINATION

George A. Hart, Douglas G. Youmans, Michelle A. Thomas
Schafer Corporation
321 Billerica Road, Chelmsford, MA 01824

ABSTRACT

The direct detection 3D imaging laser radar developed by BMDO under the DITP effort and currently being integrated for a demonstration test flight in FY2001 has the capability of significantly improving the P_K of an interceptor by providing substantially enhanced discrimination. This is especially true for threats of high interest where closely spaced objects defeat the capability of passive sensors to discriminate based on intensity modulation due to coning. The DITP 3D ladar can easily resolve such CSO's, it also has an inherent advantage in that the same amount of coning will result in 3 times as much modulation as the passive sensor would observe. The 3D ladar can also observe the actual object orientation once it is angularly resolved. This can cut through confusion the passive sensor could experience where different combinations of aspect and coning angle can yield the same modulation amplitude.

The ability of the 3D ladar to deliver such benefits hinges on the accuracy of its intensity measurements. This paper will present analysis backed by experiments, which indicates that while speckle is a potential problem, the intensity fluctuations it introduces can be mitigated by multi-pulse averaging. Sufficient engagement timeline exists for such an approach when proper trades between pulse energy, rep rate, and beam profile are made. Such trades will be presented in detail, as will the proper method for estimating the extent of speckle expected for an overall target, individual range bin, or single angle-angle pixel within a range bin.

1.0 INTRODUCTION

The BMDO Discriminating Interceptor Technology Program (DITP) is developing sensor systems to provide enhanced seeker and guidance capability against postulated advanced NMD/TMD threats[1-4] . These systems include multicolor infrared imaging detectors, laser radars, tracking and discrimination software, and a fusion processor. The laser radar is required to provide high-resolution imagery and track data for discrimination of threat objects from decoys and debris. During the past several years both coherent and direct-detection laser radar designs and hardware concepts have been evaluated for use in DITP. Recently the direct-detection solid-state laser radar was selected by BMDO/DITP for integration as a space-qualified 5-kg package as part of a demonstration flight in FY2001 which will also include a DITP advanced passive sensor system and fusion processor. Although the direct-detection system does not provide direct Doppler measurement, the other advantages of the direct-detection system, including compactness, processing simplicity, and experimentally demonstrated robust discrimination performance against representative targets, provide BMDO with a near-term laser radar for such space-based demonstrations

The BMDO DITP scenario envisions a ground-based interceptor launched at an approaching threat cloud. The threat cloud may consist of one or more RV targets and as many as 10 or 20 lightweight decoys and randomly shaped deployment debris objects. The decoys closely resemble the RVs in shape and exterior surface properties, but are perhaps 1-5% of the RV mass. Since the static optical properties of the two target sets are quite similar, the laser radar is used to measure differences in dynamics of decoy vs. RV.

Form SF298 Citation Data

Report Date *("DD MON YYYY")* 00001999	**Report Type** N/A	**Dates Covered (from... to)** *("DD MON YYYY")*

Title and Subtitle DITP 0.5 µM Imaging Ladar Target Speckle Statistics and their Impact on Discrimination	**Contract or Grant Number**
	Program Element Number
Authors	**Project Number**
	Task Number
	Work Unit Number
Performing Organization Name(s) and Address(es) Schafer Corporation 321 Billerica Road Chelmsford, MA 01824	**Performing Organization Number(s)**
Sponsoring/Monitoring Agency Name(s) and Address(es)	**Monitoring Agency Acronym**
	Monitoring Agency Report Number(s)
Distribution/Availability Statement Approved for public release, distribution unlimited	
Supplementary Notes	
Abstract	
Subject Terms	
Document Classification unclassified	**Classification of SF298** unclassified
Classification of Abstract unclassified	**Limitation of Abstract** unlimited
Number of Pages 22	

2.0 INTENSITY MODULATION

One of the most important differences in dynamics between RV's and decoys is the coning angle (precession angle). When used as weapons of terror against an extended urban area there is no need for precision targeting of RV's and measures such as spin stabilization are not necessary. But any attempt to destroy U.S. retaliatory strike capability requires precisely targeted counterforce weapons whose attitude upon reentry must be carefully controlled. For precise targeting, RV's are deployed with as small a coning (or precession) angle as possible, where deflection by the atmosphere on reentry is minimized by orienting the RV so that its body symmetry axis is co-aligned with the velocity vector it will follow on the downward sweep part of its trajectory. The large mass of the RV, careful balancing of that mass, and precision deployment by the post boost vehicle (PBV) results in a spin stabilized motion with relatively low coning. Coning angles of 2-4 degrees are typical. This is a representative value not derived from any specific threat document.

Heavy and light decoys on the other hand simply do not have the mass required to achieve and sustain such small coning angles. Even with concerted efforts towards careful balancing and deployment, medium weight "precision" decoys end up with coning angles around 8 degrees. Light replicas exhibit coning angles of approximately 12 degrees. Conical lightweight balloons will have even greater coning angles.

A direct detection laser radar, such as that to be used in the DITP FY2001 demo flight, can exploit this difference in dynamical behavior as a discriminant, because such coning produces a sinusoidal variation in the signal returned to a laser radar as the RV completes one coning cycle with a period from a few seconds to a few tens of seconds. By revisiting the RV anywhere from 5 to 10 times during its coning cycle, the direct detection ladar can determine the extent of fluctuation or modulation during that cycle. Knowledge of that modulation depth or amplitude can be translated into a determination of the coning angle.

It should be strongly emphasized that over most of its discrimination engagement timeline the laser radar is collecting this intensity modulation data. Depending on the reflectivity of the target, useful modulation measurements can begin to be made at ranges from 400 to 450 km. Up until ranges less than 200 km the aperture sizes which an interceptor aperture can accommodate (of the order of 25 cm) do not make available the necessary angular resolution for full 3D imaging. Therefore other features for measuring precession and orientation are simply not accessible for the majority of the engagement fly-in. In several scenarios it is desirable to reach a final target selection decision by approximately 150 km to allow sufficient time to reach the target given realistic interceptor divert capabilities. At a nominal NMD closing velocity of 10 km/s, 20-25 seconds will be spent making intensity modulation measurements, while typically 5, or at the most 10, seconds will be involved in full 3D imaging. This underscores the importance of the reliability of intensity modulation as a discriminant and the impact of speckle statistics and other considerations on that reliability. Before turning to an examination of error sources which must be considered in making intensity modulation measurements, it is useful to have a thorough understanding of the source of the modulation, its expected magnitude, and the special advantages an active rather than passive sensor has in observing such modulation.

From the point or view, literally, of an oncoming LADAR equipped interceptor, coning motion produces a cyclical variation of the net aspect angle between the line of sight to the threat object and that object's body symmetry axis. For example for a cone with a mean aspect angle of 30 degrees and an 8 degree coning angle the effective aspect angle will swing from 38 degrees down to 22 degrees and back up to 38 degrees over the time of one coning (precession) cycle.

This change in aspect angle is very apparent to the laser radar because it produces a corresponding and substantial change in the laser radar cross section. For a cone this cross-section has a minimum at a head on orientation. It has its maximum at 90 degrees. (Actually its maximum will be at 90 degrees minus the cone half angle. At this point one side of the cone will be exactly perpendicular to the LADAR line of sight. This "glint" line will be returned to in a subsequent discussion of moment-of-inertia algorithm[5,6] (M-O-I) determination of the threat object orientation). In going from 0 degrees to 90 degrees the cross section is given by an S shaped curve like the sine function. As shown in Figure 1 for aspect angles between 10 and 60 degrees this curve is very linear[7]. It is this linear dependence of cross section on aspect angle which produces the intensity modulation discrimination feature.

As is depicted in Figure 1, for a mean aspect angle of 30 degrees and a coning angle of 8 degrees there will be a 60 percent increase or modulation of the returning laser radar signal as the instantaneous aspect varies from 22

degrees to 38 degrees. This behavior was confirmed in experimental measurements made at the AMOR test facility in December 1997[6]. The degree of modulation is independent of the target reflectivity on ladar output power, but the signal to noise ratio depends on these two quantities together with the speckle statistics which form the core of this analysis. Before turning to those critically important photon statistics, it is instructive to note that for the same target behavior (30 degree mean aspect angle, 8 degree coning angle) only 18 percent modulation in the target's emissivity area product occurs. Where the "signal" of interest is in fact intensity modulation, the ladar thus has a factor of three advantage over the passive sensor. The ladar also benefits from the advantages of active illumination whereas the passive sensor must contend with cold targets which can challenge the sensitivity and noise characteristics of passive arrays and their associated optics. It can also be seen that the aspect angle region where modulation is useful only extends from 15 to 50 degrees for the passive sensor.

But far more important in this comparison of ladar and passive sensor capability to reliably measure intensity modulation is the problem of closely spaced objects (CSO's). For targets which are well separated and warm enough to provide adequate passive sensor signal-to-noise, the passive sensor could autonomously determine the intensity modulation. But passive sensor pixels are typically of the order of 50 μr and the blur spot for 10 micron radiation with a typical interceptor aperture of 25 cm is 100 μr . Objects within 50-100 μr cross range at 400 km (20-40 meters) are CSO's, and the summed signals from their individual coning behavior can present an impossible puzzle for the passive sensor to untangle. Many threats of high interest are heavily populated with such CSO pairs.

But with a wavelength $1/20^{th}$ of 10 micron radiation the active sensor at 532 nm using the same a 25 cm aperture has an individual pixel blur spot diameter of 5.2 μr corresponding to 2 meters at 400 km for each pixel in its 10 x 10 array. The 20 cm range resolution of the ladar can further assist in isolating one object from another in conducting these critically important intensity modulation measurements. Beyond the strongly enhanced confidence in target designation which the ladar can provide, with concomitant significant reductions in needed interceptor launches per kill (at least a factor of 3), the essential benefit the ladar introduces is the ability to perform discrimination in CSO circumstances where the passive sensor simply cannot.

There is an additional source of potential confusion which can defeat intensity modulation based discrimination by the passive sensor alone even in the absence of closely spaced objects. As is depicted in Figure 2 there are various combinations of coning angle and aspect angle which can produce the same percent modulation. For example a 4 degree coning angle at a mean aspect angle of 15 degrees will produce 37 percent modulation. But this same 37 percent figure could arise from 8 degree coning at a mean aspect angle of 6 degrees or 8 degree coning at a mean aspect angle of 41 degrees. This degeneracy can only be clarified by directly observing the aspect angle of the target. The direct detection 3D imaging ladar can do this once it is able to angularly resolve the target. This becomes possible at 200 km or less range to the target when the receiver electronically zooms its intensified photo diode detector to shift to 2.6 μr Rayleigh pixels. By applying the Moment-of-Inertia algorithm the apparent "azimuth" and "elevation" of the target can be determined to a one sigma one axis uncertainty of approximately 2 degrees. This was also demonstrated in the December 1997 AMOR field tests of the direct detection system[6]. Once so angularly resolved it is possible to observe the coning motion in stop motion snapshot fashion throughout whole precession cycles in this way. But engagement timeline considerations make this impossible to accomplish.

What can be done, however, is to quickly establish which of the three "degenerate" cases in the example being considered is actually responsible for the observed modulation. An effective strategy would be to make such an orientation angle measurement at the time when the modulation would be expected to be halfway between its peak and minimum values, at the "zero crossings." This is easy to predict from the angularly unresolved measurements of modulation made between 450 and 200 km which provide a time history from which the amplitude, period, and phase of modulation can be determined. At the moment of "zero crossing" modulation, the net aspect angle resulting from the coning angle adding to the mean aspect angle would be momentarily equal to the mean aspect angle, or 8, 15 or 41 degrees for the three cases under consideration. These values would be easily distinguishable. There are two zero crossing observation opportunities per coning cycle which eases the issue of scheduling measurements. As further confirmation measurements could be made at the time of minimum modulation where the net aspect angle is the mean aspect angle minus the coning angle or 6-8 = -2, 15-4 = 11, 41-8 = 33 for the three possible degenerate cases in this example. Again, these are easily distinguishable. A similar approach could be taken at the time of maximum modulation.

It should be emphasized that in most cases there will not be a need to use 3D imaging extraction of orientation angles to break degeneracies arising from intensity modulation measurements. As illustrated in Figure 2,

8 degree coning will most often produce 50 to 80 percent modulation which is easily separable from the maximum of less than 40 percent modulation seen for 4 degree coning at any aspect angle. But if because of variation in deployment and a resulting spread in decoy aspect angles a handful of objects display modulation resembling that from an RV, the ladar can distinguish decoys from the RV once the objects become angularly resolved. In addition because of the aforementioned purpose of spin stabilization and careful deployment for precise targeting, the orientation of the RV with respect to its velocity vector at any point in its trajectory may be well known on an a priori basis. The orientation angle measurement capabilities of the 3D imaging direct detection laser can thus provide further confidence enhancing confirmation, thereby increasing the net system P_K per interceptor launched.

As an aside, it should be noted in Figure 2 that no modulation is seen for a head-on encounter even if the target is coning. While coning will change the orientation, the net aspect angle remains the same. For lethality reasons an encounter other than head-on is preferable. As a practical matter actual scenarios of interest produce aspect angles between 20 and 40 degrees.

A more important consideration arising from Figure 2 is also directly related to the probability of a successful kill per interceptor launched. At a mean aspect angle of 30 degrees the modulation intensity is 25 percent for 4 degrees coning and 60 percent for 8 degrees coning. If each measured as 25 ± 7 and 60 ± 7 where the ± 7 denotes the standard deviation values, the difference in means divided by the root sum squared standard deviations would be $(60-25)/\text{sqrt}\ (49 + 49) \cong 35/10 = 3.5$. This would be the so-called K factor for discrimination between these two classes, and is a measure of the confidence of separability. It increases with the "distance" between the distinguishable features and decreases as measurement uncertainty blurs that distinction.

Uncertainty in the overall estimate of modulation intensity arises from the uncertainty in individual measurements the laser radar makes at successive points during the precession cycle. As mentioned above the ladar has an observation period of approximately 20 seconds in which to gather intensity measurements from which modulation parameters (amplitude, period, and phase) are extracted. The precession period can vary between 5 and 30 seconds depending on the threat, so anywhere from 4 full coning cycles down to 2/3 of one cycle will occur during this 20 second window. As the sinusoidal variation of the signal is observed the ladar must accumulate enough samples to accurately determine the sine wave's amplitude and period.

At least 4 or 5 measurements should be made during the precession period, and each measurement should be accurate enough in terms of determining intensity so that the error bars on the individual measurements do not seriously degrade the quality of the sine wave fit to the data.

For a 10 second period this would translate into one measurement every 2 seconds. It will take of the order of 20 laser pulses to obtain an individual measurement of sufficient quality as will be discussed below. At a 100 Hz rate this will allow for 5 measurements per second. As a result 10 targets can be addressed with 5 measurements every 10 seconds.

The question of optimal allocation strategies for the available laser pulses will be addressed in a subsequent section, but two points regarding implementation warrant noting here. The first is that the requirement for 4 or 5 measurement points in each pixel applies for the most challenging case where no a priori knowledge is available concerning the period or the phase of the modulation. For those targets where confusion due to the presence of another CSO is not an issue, cueing by the passive sensor can be a very valuable form of sensor fusion in instructing the ladar exactly when to make its measurements on a given object to achieve maximum benefit. As previously discussed the active sensor will often have a factor of three greater modulation to work with, thereby enhancing discrimination potential. The passive sensor could indicate to the active sensor the times when the modulation would hit its maximum and its minimum, so that only two measurements per precession cycle would be necessary. The passive sensor in non CSO cases can do a sufficiently accurate job of determining period and phase, which are not the primary quantities of interest to discrimination. The ladar can then confirm and refine the passive sensor's estimate of the modulation amplitude.

Returning to the example of targets with a 10 second coning period, if only 2 measurements per precession period were required (one every 5 seconds), with each taking 20 laser pulses, or 1/5 second, 25 targets could be addressed. More likely some hybrid approach would be employed, where this fused cueing would be used when the passive sensor had a high confidence estimate of a non-CSO object's period and phase, while the more measurement intense 4 to 5 ladar samples per period would be directed at those objects which were CSO's or otherwise confusing

to the passive sensor. As a result anywhere from 10 to 25 objects could be addressed depending on the possible extent of cueing of the ladar by the passive sensor.

This approach becomes important if the target coning period can be as short as 5 seconds, for here one measurement per second would be needed without cueing, and one every 2.5 seconds with cueing. From 5 to 12 objects could be treated depending on the fraction of objects which could be cued. This number of objects addressed might be increased by as much as a factor of 2 because data on more than two periods is probably not necessary, and this would mean then an individual object need not be interrogated for the full 20 seconds flight time between 400 and 200 km range. A 10 second observation window per object would be sufficient.

The second point regarding implementation worthy of note here is that the current 100 Hz, 250 mJ per pulse operating parameters of the ladar are most likely not yet fully optimized. Originally for the direct detection ladar option, DITP had envisioned 50 Hz, 500 mJ operation, but analysis of the impact of speckle statistics on measurement quality, as is discussed subsequently, made it clear that as long as initial acquisition range were not penalized severely, it was beneficial to trade joules per pulse for repetition rate. That trade perhaps should be pushed further, or a pulse energy/rep rate agile mode of operation developed which can adjust this trade during fly-in. The 25 watt average power of the ladar is also not an inflexible figure which cannot be adjusted upwards. Weight, power and volume efficiencies were gained in going to fewer joules per pulse which could open the path to a higher rep rate at the same joules per pulse in subsequent ladar designs.

There are several potential sources of error for each measurement of intensity during a precession cycle. There is shot noise including speckle, intensity variation due to the target being in a different section of the outgoing Gaussian laser beam from one measurement to the next, and power variation in the laser itself.

Laser power variation has been measured to be no more than 1 to 2 percent over much longer periods than an interceptor engagement would involve. As an additional safeguard against this unexpectedly becoming a non-negligible error source, it is planned to measure outgoing laser power on a shot to shot basis to detect any problems and, if necessary, serve as a normalizing factor.

If a Gaussian laser profile is used, it is necessary to position the object whose reflected intensity is being measured at the center of the beam. Each time the target is reacquired it must be pulled to center. The outgoing laser beam has a $1/e^2$ diameter of 52 μr spanning 20 meters at 400 km. Some number of shots, currently assumed as 3, will be required to effect this centering. There is a presumption in this that the ladar detector and outgoing laser beam are perfectly aligned. After the stresses of launch this may not be the case, and at present DITP is carrying a worst case uncorrected boresight offset of up to 7.5 μr for these two components. This could only exact a penalty of 15% as compared to being at true beam center, and would be replicated revisit to revisit, thereby not serving to corrupt the intensity measurements. However jitter about this position could compromise intensity measurements, if the jitter magnitude and time characteristics were such that it served to introduce undesirable intensity variation. This has been the subject of thorough analysis and for jitter value of 1 sigma 1 axis of 5 μr or less is negligible. An alternate approach, which will be subsequently discussed, would be to erect a top hat rather than a Gaussian in the far field. This avoids the three shot overhead required for centering and removes the concern with jitter. However it imposes a factor of three penalty in terms of intensity reduction. Detailed trades are still underway to establish which is the more promising path. At present the Gaussian approach still has the upper hand. Primarily because it is preferable to make fewer high quality measurements during a precession cycle (using ~20 laser pulses each) rather than more low quality measurements (with 1-4 laser pulses each). If the latter approach were preferable, then the 3 pulse centering overhead would be unacceptably burdensome. For 20 pulse measurements this is not the case.

What drives the need to use 20 laser pulses rather than 1 for a usable measurement of intensity is the large shot to shot variation, 30-70 percent in relative intensity, which is inherently involved in photon emission which is a random process. In the limit of very low photon counts, of the order of 1 per detection period, the variation is primarily described by Poisson statistics where the variance is given by $\sigma^2 = N_s$ and the standard deviation is given by $\sigma = (N_s)^{1/2}$ where N_s is the mean number of photons, or photoelectrons after conversion by a detector. For $N_s = 1$, which is representative of the <u>total</u> target return at ~450 km range, the standard deviation is equal to the mean so that the relative accuracy of a single laser pulse measurement would be $\sigma/N_s = 1$ or 100 percent relative error. In addition to this inherent shot noise, which would characterize emission or reflection from any source, ladar intensity measurements may be corrupted by target surface produced "laser speckle". Here reflections from various regions of

the surface produce small zones of coherence which can interact with other such subareas in "mutual coherence". In this way these subareas can either constructively or destructively reinforce to produce outgoing irregularly shaped regions, rays, or beamlets of either greater or lesser intensity producing a mottled or "speckled" appearance of the target as viewed at a distant aperture. The number of such light and dark pairs, or speckle cells, is given by M, the mean number of speckle cells in the aperture. Involving self-interaction of the reflected light, speckle is an inherently non-linear process and the variance associated with its effect is given by $\sigma^2 = N_s^2/M$.

M includes speckle cells from both polarizations when the illuminating laser includes both, or when the target depolarizes an incoming beam upon reflecting it. In support of the DITP program an exact computational method was developed to calculate the mean number of speckle cells appearing in the aperture[8]. The often used approximate formula for this quantity is [9]

$$M = 1 + (A_s A_r)/(\lambda^2 R^2) \quad (1)$$

where A_s is the area of the source region, A_r is the area of the receiver aperture, λ is the wavelength, and R is the range to the target.

The central topic of this paper is the effect of laser speckle on the accuracy of intensity measurements made to determine the intensity modulation due to coning as a critical discriminant. At the long target ranges of interest to DITP, the small target source regions, particularly per voxel (range-bin per angle-angle pixel, or per 3D pixel), result in large speckle sizes back at the ladar receiver. M per voxel is typically 2-4 for both polarizations. This can produce strong fluctuation in the signal per voxel depending on the intensity of the light captured by the detector from the small source regions.

However for very small source areas, and especially for non-contiguous areas of any size (e.g., an annulus) the approximation of Equation 1 can underestimate the true M value given by a rigorous wave optics treatment. Such an underestimation could have a negative impact on assessments of potential system performance because it would suggest greater intensity uncertainty than is actually present. This in turn would indicate more laser pulses were needed to ensure discrimination feature accuracy thereby stretching out the time required to characterize each threat object. Timeline effectiveness is critically important to the DITP mission.

The M values characterizing the DITP engagement for targets of interest will be described in detail, as will the mean number of photoelectrons per voxel. This latter quantity is important because for typical DITP M values per voxel (M=2-4, dual polarization) if $N_s < 1$, Poisson behavior dominates, and speckle becomes a secondary perturbation. Once N_s/voxel approaches 4-10, speckle effects become of prime importance.

If the photon statistics are non-Poisson (negative binomial), careful attention must be given to the precise fashion in which expected intensity fluctuations from different voxels are added together to yield the total intensity fluctuations for a given range bin, or total intensity fluctuations for the entire target. Negative binomial distributions do not simply sum the way the normal and Poisson distributions do in producing a cumulative distribution from contributing components. This becomes important in deriving a total target return in the angularly unresolved case from the photons in each range bin as they are added together. Here, as previously discussed, the modulation of the total return is a valuable means of determining target coning angle, but only if this modulation is not masked by photon statistics noise. In the angularly resolved case the contributions must be summed over both angle-angle pixels and range in deriving a total photon return whose statistics must not be so noisy as to obscure reliable modulation information. Similarly the summation over angle-angle pixels in a given range bin needs to produce a total for that range bin which can be used to reliably determine the range-sliced intensity profile of the object in questions.

Under DITP sponsorship an exact technique has been developed for calculating the number of speckle cells returned to a receiver aperture from a target illuminated by a ladar. This number of speckle cells, the M value, has a direct impact on the shot to shot fluctuation in the intensity returned to each 3D pixel (voxel), each range bin, and from the target as a whole in a 3D imaging ladar. As previously discussed, when N_s is the number of photons (or equivalently photoelectrons after photon conversion by the detector) the standard deviation of the intensity taking into account Poisson shot noise and speckle effects is given by

$$\sigma = (N_s + N_s^2/M)^{1/2} \quad (2)$$

For many situations of interest to DITP the reflecting area of the target will not have a simple rectangular or circular disk shape. Those are the only cases previously treated in detail in the literature where the assumption of uniform illumination was usually made[10-12]. The BMDO DITP funded effort has completely generalized the computational method for M, fully and rigorously treating the mutual coherence effects responsible for speckle. These effects are diffraction-like in their dependence on the shape of the reflecting surface, and especially so if that shape has any open or non-reflecting areas. Annular regions produce M values far larger than would be expected on the basis of their area alone.

Beyond developing a previously unavailable method for obtaining critically important M values, this study also has established how such M values for separate range bins of a target can be summed to yield the M value for the target cross section as a whole Moving in the opposite direction, how such an M value for the target area appearing in a given range bin should be apportioned over the multiple detector angle-angle pixels which may view that area was determined. Neither the summing nor apportioning methods were previously available. Consequently the methodology developed here represents a significant advance not only to the DITP solid state ladar direct detection approach but also to all similar 3D imaging applications where speckle is an important consideration.

The M-value summing method developed by Youmans can be used for three types of summing: summing angle-angle pixels within a given range bin; summing contributions from different range bins; or summing intensities in a given 3D-pixel (voxel) captured over several laser pulses or “shots."

For the M value summing technique to be strictly applicable the terms which are combined must be from regions which are uncorrelated in terms of speckle lobes. For 2D pixels this is satisfied when the individual pixel centers are separated by at least 2.44 λ/D. More accurate results are obtained when the pixel separation is 4.88 λ/D. For Rayleigh pixels of 1.22 λ/D separation adjacent pixels are highly correlated in many cases with respect to the speckle lobes which are viewed, especially when the mean number of speckle lobes per pixel, denoted by M, is $M \leq 10$.

As a consequence the initial simple summation procedure suggested by Youmans where pixels are summed together to yield a net negative binomial distribution whose effective M value is given by

$$M_{eff} = \sum_i M_i . \qquad (3)$$

such an approach to summing over the pixels in a given range bin can produce an erroneously high value of M_{eff} if the speckle cells in adjacent pixels are correlated. The same can be true for summing M values over adjacent range bins if the coherence time τ_c is such that $c\tau_c/2$ is greater than the range bin depth.

There is another potential problem in the simple M value summation even when the pixel speckle cells are uncorrelated. That arises from the fact that the "floor" on M is 1, indicating that M is never expressed as a fraction of a speckle cell or lobe. But in summing to an M_{eff} this "floor" will potentially make the total M value several times greater than it should be.

In the pixel summing case where speckle cell correlation or the M value floor of 1 can be a problem, the approach which should be taken is to evaluate the M value for the entire area within a range bin. This is the true M_{eff} . As has been discussed above and is treated in depth in another paper, this M_{eff} calculation must carefully take into account diffraction effects not considered by the commonly used approximation for M given in Equation 1. Once the M_{eff} value has been properly computed it should be apportioned to the individual pixels contributing to it.

Here another assumption implicit in Youmans' initial memo on M value summation emerges as important. His memo assumed that each source area was emitting or illuminated with the same intensity per square meter. In many situations of interest this will not be the case. The M_{eff} should be apportioned on the basis of the fraction of the total intensity emanating from each pixel. If this fractional apportionment would produce an M value less than one, the previously discussed floor of one should be applied.

The way to apportion the M_{bin} for the entire illuminated area in a given range bin to the individual pixel viewing that area is

$$M_{pixel} = \max\left(\frac{N_{pixel} M_{bin}}{N_{bin}}, 1\right) \tag{4}$$

where M_{pixel} is the speckle M value for an individual pixel, N_{pixel} is the intensity in that particular angle-angle pixel and N_{bin} is the total intensity in a given range bin. This is a single polarization result and should be multiplied by two to account for two polarizations.

The method for accumulating the total M_{target} for multiple range bins where the coherence length is not greater than the range bin depth is to weight the contribution of each range bin by the total intensity in that bin compared to the bin with the greatest intensity

$$M_{target} = \sum_{bins} \frac{N_{bin} M_{bin}}{N_{max\,bin}} \tag{5}$$

where M_{target} is the net M value for the target taken as a whole, N_{bin} is the intensity in a given range bin, M_{bin} is the speckle cell number for that bin, and N_{max} bin is the intensity of the bin with the greatest reflected illumination. Equation 5 will be used repeatedly in a subsequent discussion of representative target M values at different ranges and aspect angles.

One of the instances where the most simple version of the Youmans' M value summation method, Equation 3, can be used is for the case of a total target, individual range bin, or single 3D pixel (voxel) where multiple shots are accumulated to reduce the uncertainty in measured intensity. This issue of intensity accuracy expressed as σ_{Ns}/N_s arises due to the requirements of various discrimination algorithms. Intensity modulation as an indication of precession angle requires about ten percent intensity accuracy (relative, not absolute) while the moment-of-inertia algorithm as a source of shape and orientation information is more forgiving. It requires about forty percent relative accuracy. Youmans' formulae

$$N_{s-eff} = \sum_i N_{si} \tag{6}$$

$$M_{eff} = \sum_i M_i \tag{7}$$

apply directly to this shot summation case for a total target, individual range bin, or single voxel. There are some algebraic manipulations which can be applied to the resulting expression for standard deviation which are extraordinarily useful in system effectiveness assessment and timeline determination.

For a single shot

$$\sigma_{1-speckle} = (N_s + N_s^2 / M)^{1/2} \tag{8}$$

For n multiple shots

$$N_{s-eff} = \sum_i N_{si} = nN_s \tag{9}$$

$$M_{eff} = \sum_i M_i = nM \tag{10}$$

so that

$$\sigma_{eff-speckle} = (nN_s + n^2 N_s^2 / nM)^{1/2} \tag{11}$$

$$= n^{1/2}(N_s + N_s^2/M)^{1/2} \tag{12}$$

$$= n^{1/2}\sigma_{1-\text{speckle}} \tag{13}$$

where $\sigma_{1\text{-speckle}}$ is the standard deviation for a single shot.

The quantity of most interest is

$$\frac{\sigma_{\text{eff}}}{N_{s-\text{eff}}} = \frac{n^{1/2}\sigma_{1-\text{speckle}}}{nN_s} = \frac{1}{n^{1/2}}\frac{\sigma_{1-\text{speckle}}}{N_s} \tag{14}$$

This is precisely the $(1/n^{1/2})$ reduction in relative error from multiple shots dependency seen in the case of Poisson statistics where

$$\sigma_{1-\text{Poisson}} = (N_s)^{1/2} \tag{15}$$

where 1-Poisson denotes a single shot for a Poisson case and N_s is the single shot intensity, and

$$\frac{\sigma_{1-\text{Poisson}}}{N_s} = \frac{1}{(N_s)^{1/2}} \tag{16}$$

Multiple shots in the Poisson case produce

$$N_{s-\text{eff}} = nN_s$$
$$\frac{\sigma_{\text{eff}-\text{Poisson}}}{N_{s-\text{eff}}} = \frac{1}{(nN_s)^{1/2}} = \frac{1}{n^{1/2}}\frac{\sigma_{1-\text{Poisson}}}{N_s} \tag{17}$$

This similarity of dependency is shown in Figure 3.

There is a " penalty factor" to be applied in going from the Poisson to the speckle case in terms of more shots being required. This penalty factor", pf, can be computed exactly.

To make the relative accuracy of the speckle case after n shots equal that of the Poisson after one shot set

$$\frac{\sigma_{1-\text{Poisson}}}{N_s} = \frac{\sigma_{n-\text{speckle}}}{nN_s} \tag{18}$$

$$\frac{(N_s)^{1/2}}{(N_s)} = \frac{(nN_s + (nN_s)^2/nM)^{1/2}}{nN_s} \tag{19}$$

$$(N_s)^{1/2} = \frac{n^{1/2}(N_s + N_s{}^2/M)^{1/2}}{n} \tag{20}$$

$$n = (1 + N_s/M) = \text{ppf} \tag{21}$$

Here n is the number of shots required, and represents the multiplicative "photoelectron penalty factor" ppf introduced by considering speckle. It represents how many times more total photoelectrons are required due to speckle compared to those for a pure Poisson case to achieve the same level of relative accuracy. For N_S=4 and M=2 ppf =1+2=3 = n. So three shots in the speckle case will be necessary.

$$\frac{\sigma_{1-\text{Poisson}}}{N_s} = \frac{(N_s)^{1/2}}{N_s} = \frac{2}{4} = .5 \tag{22}$$

$$\frac{\sigma_{3-\text{speckle}}}{3N_s} = \frac{\left(nN_s + (nN_s)^2 / nM\right)^{1/2}}{nN_s} = \frac{(12 + 144/6)^{1/2}}{12} = \frac{6}{12} = .5 \tag{23}$$

For N_s = 2 and M = 2 ppf = 1+1 = 2 = n

$$\frac{\sigma_{1-\text{Poisson}}}{N_s} = \frac{(2)^{1/2}}{2} = \frac{1}{(2)^{1/2}} \tag{24}$$

$$\frac{\sigma_{n-\text{speckle}}}{nN_s} = \frac{(4 + 16/4)^{1/2}}{4} = \frac{1}{(2)^{1/2}} \tag{25}$$

For N_s = 1 and M = 2 ppf =1 + .5 = 1.5. For a numerical example to make sense compare the case where m Poisson shots are accumulated and 1.5 m is an integer as for m = 2 and 1.5 m = 3.

$$\frac{\sigma_{2-\text{Poisson}}}{2} = \frac{(2)^{1/2}}{2} = \frac{1}{(2)^{1/2}} \tag{26}$$

$$\frac{\sigma_{3-\text{speckle}}}{3} = \frac{(3 + 9/6)^{1/2}}{3} = \frac{\left((6+3)/2\right)^{1/2}}{3} = \frac{1}{(2)^{1/2}} \tag{27}$$

For N_s = .5 and M = 2 ppf = 1 + .25 = 1.25. Compare m=4 Poisson shots (N_s = .5 per shot) with n=5 speckle shots (N_s = .5 per shot).

$$\frac{\sigma_{4-\text{Poisson}}}{2} = \frac{\sqrt{2}}{2} = .707 \tag{28}$$

$$\frac{\sigma_{5-\text{speckle}}}{2.5} = \frac{(2.5 + 6.25/10)^{1/2}}{2.5} = .707 \tag{29}$$

It can thus be seen that this "penalty factor" approach is applicable to N_s values greater than, less than or equal to one.

In arriving at the equation ppf= (1 + N_s/M) it was assumed that $N_{Poisson}$ = $N_{speckle}$ = N_s the mean number of photoelectrons per shot. To more transparently handle the general case where $N_{Poisson}$ is not equal to $N_{speckle}$ another expression can be derived. This is useful because the Poisson case is so easily handled when $N_{Poisson}$ is set equal to one. Then for example it is immediately apparent that for ten percent relative accuracy one hundred shots are needed, and for one percent accuracy ten thousand shots are required. It is desirable to be able to immediately translate such shot counts into a speckle case for M = 2 (the nominal DITP value per voxel) with $N_{speckle}$ = 0.6, 1.2, 3.8, etc. mean photoelectron counts per measurement.

A given fractional relative error P (e.g., 0.10 for 10 percent) can be achieved for the Poisson case by averaging over multiple shots so as to accumulate m photoelectrons. The relative error for that total is given by

$$\frac{\sigma_{m-\text{Poisson}}}{m} = \frac{m^{1/2}}{m} = \frac{1}{m^{1/2}} = P \tag{30}$$

The total required Poisson photoelectrons m is thus equal to the well known result $1/P^2$. Applying the penalty factor, ppf = $(1 + N_s/M)$, gives the total number of photoelectrons required in the speckle case

$$PE_{tot} = pf / p^2 = (1 + N_s / M) / P^2 \tag{31}$$

The number of shots n in the speckle case to produce P fractional relative error is thus given by

$$n = PE_{tot} / N_s = (1/N_s + 1/M) / P^2 \tag{32}$$

$$n = (1/P^2)\,(1/N_s + 1/M) \tag{33}$$

If speckle were negligible, M = ∞, this would reduce to

$$n = (1/P^2) / N_s \tag{34}$$

and would describe the Poisson case with N_s photoelectrons per shot. The additive 1/M term in Equation (33) causes the need for additional shots. If M = ∞ there is no penalty for going to larger photoelectrons per shot N_s. But as M approaches 1 the 1/M term can come to dominant the $(1/N_s + 1/M)$ factor unless N_s is comparably small. From a system point of view it would be energetically wasteful to have a large N_s per pulse and yet have the 1/M term call for as many pulses as if N_s were small. To keep the speckle "penalty" in check from the point of view of the number of shots required for an intensity measurement of given accuracy, it is advisable to keep $1/N_s$ four or more times greater than 1/M, or $N_s/M \leq .25$. This analysis in terms of shots required relates back to the "photoelectron penalty factor" of Equation 21 $(1 + N_s/M)$. Operationally it means that a ladar may be far more efficient operating at a higher rep rate and lower energy per pulse. To turn that assertion into useful engineering guidance requires accurate estimates of the M values for the total target, individual range bins and single voxels together with the expected return from the target based on geometry and reflectivity.

Applying $n = (1/P^2)\,(1/N_s + 1/M)$ to a DITP issue of high interest will illustrate the utility of this expression. Consider a situation where ten percent relative accuracy of the intensity estimates is required for four different N_s values 0.5, 1, 2 and 4. The N_s=1 Poisson case would necessitate 100 shots. Here M=2 is assumed.

Table 1

$\bar{N}_s$ (M=2)	0.5	1	2	4	8	16	32	64
$(1/N_s + 1/M)$	2.5	1.5	1	0.75	0.625	0.5625	0.53125	0.515625
Shots	250	150	100	75	62.5	56.25	53.125	51.5625
EnergyRequired = shots x N_s	125	150	200	300	500	900	1700	3300

For the Poisson case where M = ∞ this table would become

Table 2

$\bar{N}_s$ (M=∞)	0.5	1	2	4	8	16	32	64
$(1/N_s)$	2	1	0.5	0.25	0.125	0.0625	0.03125	0.015625
Shots	200	100	50	25	12.5	6.25	3.125	1.5625
EnergyRequired	100	100	100	100	100	100	100	100

= shots x N_s								

demonstrating the well known Poisson result that photoelectrons are photoelectrons no matter how many arrive per voxel per measurement.

An important point apparent from Table 1 is that from a system design perspective it would be optimal to be able to adaptively adjust the ladar transmitter joules per pulse and pulse rate so that the mean number of photoelectrons per voxel per measurement was kept around one once the target is angularly resolved. This is where the knee in the net energy per intensity measurement requirement curve occurs. There is some additional benefit in going down to a mean value of 0.5, but only a slight advantage, and it introduces detector signal to noise problems.

Examining some examples of M values calculated for individual range bins and M value summing over those range bins to get a total target M value is probably the best way to get a firm grasp on the potential performance of the system and the system operating parameter trades under investigation.

The graph at the top of Figure 3 shows the M value per range bin for the case of a 2 x 1m cone at 200 km and 0 degree aspect angle calculated both using the standard approximation and the exact technique developed under DITP and validated by data taken in September-November 1998[13]. The graph at the top of Figure 4 is for the same conditions with 30 degree aspect angle. Figure 3 clearly illustrates the substantial difference between the standard approximation for M and the true M for the head-on cone. Although a head-on engagement is unlikely, and undesirable, a mean aspect angle of 15 degrees and a coning angle of 12 degrees will sweep through this near zero region during the coning cycle. The returning amplitude will be a minimum here, and is accordingly important in estimating total modulation and the implications of the exact M calculation method will provide significant positive system benefit.

As the graph at the top of Figure 4 indicates, at an aspect angle of 30 degrees where the reflective area in each range bin much less resembles an annulus and is much more like a solid contiguous area, the standard approximation is far more valid. Here the diffraction effects leading to the M value, enhancement seen for the head-on annuli play a much smaller role except in range bins eight and nine. Even here the effect is less than would be expected from the "annular" shape of the area because most of the intensity is concentrated around the "centerline". As discussed before the M value is an intensity weighted phenomenon.

For the purposes of discrimination using range template matching (range profiling) or intensity modulation as a means of determining precession angle and frequency, both the exact M value calculation technique and intensity weighted method for summing M values become of critical importance.

In terms of intensity modulation it is the photoelectron sum over all range bins which must be accumulated. For the head on cone case the M values of the ten annuli are added together with a weighting factor. As previously discussed that weighting factor is the intensity in a given range bin normalized to the range bin with the greatest intensity.

In the table at the bottom of Figure 3 for the head-on cone case at 200 km the computation flow is captured for calculating shots required for range template matching as well as intensity modulation. The photoelectrons per range bin are given along with the resulting weighting factor shown in column three. In this case range bin 10 had the greatest intensity and its photoelectron count becomes the normalizing divisor. The M values which would have been computed from the standard or Yura approximation are given in column four. The M values calculated exactly are given in the sixth column. It cannot be stressed greatly enough how significantly this impacts the DITP system timeline. For the range bins which most significantly contribute to range template matching and intensity modulation there is a factor of three to four enhancement of M.

The net M value for the target taken as a whole to be used in determining the uncertainty in the intensity measurement from the total cross section is arrived at by multiplying the weighting factor in column three by the exact M's in column six. These sum to a net M of 21.67. This net M is then multiplied by 2 to take into account two polarizations returned by the target. The fifth column shows the corresponding number from the standard approximation which is a factor of three smaller.

To calculate how many of these shots (each returning 20.11 photoelectrons) are required to match the 10 percent accuracy of 100 Poisson photoelectrons the expression

$$n = (1/P^2)(1/N_{s-eff})(1 + N_{s-eff}/M_{eff}) = (1/P^2)(1/N_{s-eff})pf \quad (35)$$

is used where n is the "penalty factor" due to speckle, $N_{s\text{-}eff}$ is the photoelectrons summed over all range bins (20.11) and M_{eff} is the weighted sum of M over range bins (43.34). Here, as shown in the table at the bottom of Figure 3 , $(1/N_{s\text{-}eff})pf=0.073$. So 7.3 DITP shots would be needed to produce the 10 percent accuracy which would result from capturing 100 Poisson photons. If seven shots are used

$$\frac{\sigma}{N_s} = \frac{[(7 \times 20.11) + (7 \times 20.11)^2/(7 \times 43.34)]^{1/2}}{(7 \times 20.11)} = 0.102 \quad (36)$$

To get five percent accuracy 4 x 7.3 = 29 shots would be needed.

Using similar information in the table at the bottom of Figure 4 for the 200 km 30 degree aspect angle cone case, the number of shots required for 10% and 5% intensity modulation accuracy can be determined. That would be 8 and 32 respectively.

Turning to range template matching, the tables at the bottom of Figures 3 and 4 determine the shots needed for usable data.

The second graphs in Figures 3 and 4 show the photoelectrons per range bin for the 0 degree and 30 degree aspect angle cases at 200 km. If the intensity is held to 10 percent uncertainty (standard deviation) in the range bin with greatest intensity it can be seen that a usable profile results. This ten percent standard deviation is shown on the photoelectrons per range bin curves. Also shown as separate curves are the resulting standard deviations from one shot and multiple shots, where the multiple shots are whatever number is required to produce ten percent relative accuracy in the range bin with the greatest intensity. In each instance the "penalty factor" for the most intense range bin was used to determine the number of shots required. For example in the case of the head-on cone at 200 km range bin 10 is involved. Here N_s = 3.82 and M = 5.95 (times 2 for two polarizations) so , $(1/N_{s\text{-}eff})pf$ = 0.346 and 35 shots are required.

Had the standard Yura approximation for M been used, M would have been 3.30 not 11.90 and the shot requirement would have ballooned to 56, a 60 percent increase. Analysis of the impact of speckle on the number of laser pulses needed to obtain sufficiently accurate intensity measurements during a precession cycle to use the degree of intensity modulation as a discriminant, as has just been discussed, is central to the evaluation of system effectiveness. It also is essential to determining the most suitable strategies for ladar usage. Here the question of accuracy as a function of range becomes paramount.

Table 3 extends the previous analysis of the 30 degree aspect angle, 8 percent target reflectivity, 200 km case to the entire spectrum of ranges of interest, roughly 400 down to 100 km. The ranges in Table 3 were chosen to

Table 3 Impact Of M Values On Timeline 30 Degree Aspect 8% Reflectivity

Range (km)	**365**	**300**	**260**	**210**	**180**	**150**	**120**
N_s (photoelectrons)	**4**	**9**	**16**	**36**	**64**	**144**	**324**
σ= sqrt (N_s) Poisson	**2**	**3**	**4**	**6**	**8**	**12**	**18**
σ/N_s	**.50**	**.33**	**.25**	**.17**	**.13**	**.08**	**.06**
Shots for σ/N_s = 10%	**25**	**11**	**6**	**3**	**2**	**1**	**1**
M_{exact}	**11**	**12**	**14**	**16**	**20**	**24**	**30**
σ= sqrt ($N_s + N_s^2/M$)	**2.33**	**3.97**	**5.86**	**10.82**	**16.40**	**31.75**	**61.83**
σ/N_s	**.58**	**.44**	**.37**	**.30**	**.26**	**.22**	**.19**
Shots for σ/N_s =10%	**34**	**19**	**13**	**9**	**7**	**5**	**4**

Table 4 Impact Of M Values On Timeline 16 Degree Aspect 8% Reflectivity

Range (km)	365	300	260	210	180	150	120
N_s (photoelectrons)	8	18	32	72	128	288	648
σ= sqrt (N_s) Poisson	2.82	4.24		8.49		16.9	25.46
σ/N_s	.35	.24	.18	.12	.09	.06	.04
Shots for σ/N_s = 10%	13	6	3	1	1	1	1
M_{exact}	11	12	14	16	20	24	30
σ= sqrt ($N_s + N_s^2/M$)	3.72	6.71	10.25	19.90	30.78	61.12	121.02
σ/N_s	.46	.37	.32	.28	.24	.21	.19
Shots for σ/N_s =10%	22	14	10	8	6	5	4

Table 5 Impact Of M Values On Timeline 0 Degree Aspect 8% Reflectivity

Range (km)	365	300	260	210	180	150	120
N_s (photoelectrons)	1.6	3.5	6.3	14.7	27.2	56.4	137.5
σ= sqrt (N_s) Poisson	1.26	1.87	2.51	3.83	5.21	750	11.73
σ/N_s	.79	.53	.40	.26	.19	.13	.08
Shots for σ/N_s =10%	63	29	16	7	4	2	1
M_{exact} Speckle	19	26	32	42	54	64	80
σ= sqrt ($N_s + N_s^2/M$)	1.32	1.99	2.75	4.45	6.40	10.30	19.33
σ/N_s	.82	.57	.44	.30	.24	.18	.14
Shots for σ/N_s =10%	68	32	19	9	6	3	2
M_{approx} Speckle	11	12	14	15	17	20	25
σ= sqrt ($N_s + N_s^2/M$)	1.35	2.13	3.02	5.40	8.41	14.68	29.90
σ/N_s	.85	.61	.48	.37	.31	.26	.22
Shots for σ/N_s = 10%	72	37	23	13	10	7	5

Table 6 Impact Of M Values On Timeline 0 Degree Aspect 16% Reflectivity

Range (km)	365	300	260	210	180	150	120
N_s (photoelectrons)	3.2	7.0	12.6	29.4	54.4	112.8	275.0
σ= sqrt (N_s) Poisson	1.79	2.65	3.55	5.42	7.37	10.60	16.59
σ/N_s	.56	.38	.28	.18	.13	.09	.06
Shots for σ/N_s = 10%	31	15	8	3	2	1	1
M_{exact} Speckle	19	26	32	42	54	64	80
σ= sqrt ($N_s + N_s^2/M$)	1.93	2.98	4.19	7.07	10.45	17.65	34.93
σ/N_s	.60	.43	.33	.24	.19	.16	.13
Shots for σ/N_s = 10%	36	18	11	6	4	3	2
M_{approx} Speckle	11	12	14	15	17	20	25
σ= sqrt ($N_s + N_s^2/M$)	2.03	3.33	4.89	9.32	15.12	27.37	57.45
σ/N_s	.64	.48	.39	.32	.28	.24	.21
Shots for σ/N_s = 10%	40	23	15	10	8	6	4

match points where the number of photoelectrons were the squares of integers to facilitate use of the table. The table indicates the standard deviation and relative error which would hold if Poisson statistics were applicable were $\sigma/N_s = (1/N_s)^{1/2}$. The corresponding standard deviations and relative errors are also shown when speckle is considered. Here 36 percent more up to 4 or 5 times more shots would be required as the range decreases from 365 to 120 km. This reflects the point underlined earlier that the "photoelectron penalty factor" associated with speckle is (1 + N_s/M). At 365 km M is 3 times greater than N_s and the impact of speckle is perceptible but not overwhelming. At 150 km N_s is 6 times s large as M and the impact of speckle is great reflecting its non-linear dependence on intensity.

As this would suggest, as the target reflectivity is doubled along with the number of photoelectrons at each range, the energy efficiency price exacted by speckle becomes more acute. As shown in Table 4 at 365 km N_s is 72 percent of M so 72 percent more ladar pulses are required than would be the case in the absence of speckle, 22 vs. 13. So although as expected the greater returning signal reduces the number of pulses required, the energy efficiency has dropped. This could be regained by a rep rate agile device which could drop the pulse energy and increase the firing rate, keeping the net power draw constant.

For the head-on cone case the effects of speckle are more muted because the number of photoelectrons drops by a factor of 2.5 while the M values increase by about a similar factor, decreasing the N_s/M ratio by a factor of six as is seen in Table 5. For ranges of 200 km and above there is little difference between the speckle and Poisson calculations of the number of shots required for 10 percent relative error. Below 200 km N_s becomes comparable to M and 50 to 100 percent more spots would be required.

The speckle situation would have been markedly worse at ranges less than 250 km if the M values from the standard approximation were used. This is apparent in the bottom section of Table 5. As previously discussed, experiments in September-November 1998[13] validated the exact approach for calculating the speckle mutual coherence function as a way of determining M.

As the reflectivity at 0 degrees aspect is increased from 8 percent to 16 percent in Table 6, the impact of speckle becomes pronounced (a 50% increase in the number of shots required) by 250 rather than 200 km. It's at this point that $N_s/M = 0.5$.

There are many scenario factors (target reflectivity), and system trades (laser power, rep rate, Gaussian vs. top hat beam, number of laser shots per intensity measurement, etc.), which must be considered in overall performance assessment. It is useful to assume different levels of intensity at 400 km, invoke R^4 intensity scaling, select a typical aspect angle in computing M (e.g. 30 degrees), and compute the Poisson and speckle standard deviations and relative errors. This is what is done in Figure 5 for intensity values of 2, 4 and 8 photoelectrons at 400 km. As a point of reference an 8 percent reflective, 2 x 1 meter cone, at the center of a 52 μr $1/e^2$ diameter Gaussian 250 millijoule beam for a 25 cm aperture, 40 percent quantum efficiency, 80 percent transmission efficiency and 64 percent reception efficiency will return 2.8 photoelectrons.

Of particular interest are the N_s and M curves, and the ranges where N_s first becomes equal to and then exceeds M. As previously mentioned, under active analysis is the question of whether fewer pulses per intensity measurement and more measurements rather than vice versa is optimal. The ability to do that would hinge on whether a flat top could be erected at range so that there was not a severe penalty for shots required to center the target in a Gaussian, if only a few "measurement" pulses were then to be launched. The feasibility of constructing such a flat top has been questioned. Such flatness usually comes at the expense of broadening the beam to such an extent that there is a severe intensity penalty. If the flat top radius is reduced, unacceptable "ringing" patterns could corrupt intensity modulation measurements. The width of the flat top is determined by the radius of curvature of the outgoing phase front. As is shown in Figure 6 for a beam radius at the primary aperture of 10 centimeters and a super-Gaussian parameter of 5, a phase front radius of curvature of 3500 m produces an acceptable compromise between beam width at range and flatness. Figure 7 illustrates that this beam profile extends from 100 to 400 km range.

With the relative accuracy curves of Figure 5 in hand, key implementation questions can be addressed, such as how many laser pulses should be used per intensity measurement. There are two possible approaches, either choose a fixed number of pulses and let the relative error decrease with range, or select a fixed relative error and let the number of pulses decrease with range. In either case it is useful to gauge approximately how many pulses will be required to produce useful measurements. In trying to fit a sinusoid to a series of measurements, if the measurements are of too poor quality, no matter how many there are, the fitting algorithm can be defeated altogether. The standard deviation of the individual measurements should not be more than roughly half of the modulation amplitude. As an example, for an intensity of 2 at 400 km the relative error at 300 km is 50 percent. Averaging 25 shots would push that down to 10% which would be appropriate for a 4 degree coning angle whose modulation depth is 25 percent. At 200 km the same 25 shots would decrease the expected relative error from 30 percent to 6 percent, while at 400 km the 75 percent relative error would have been reduced to 15 percent.

As previously discussed 25 shots per measurement may not fit within the engagement timeline and still permit sufficient measurements per precession cycle. Trades involving 4, 9, 16 and 25 shots per measurement does not lend itself to Fourier techniques for extracting reliable estimates of amplitude and period. Variations on the Nelder-Mead simplex algorithm are especially effective in extracting modulation parameters from measurements.

3.0 SUMMARY

The direct detection 3D imaging laser radar developed by BMDO DITP and currently being integrated for a demonstration test flight in FY2001 has the capability of significantly improving the P_K of an interceptor by providing substantially enhanced discrimination. This is especially true for threats of high interest where closely spaced objects defeat the capability of passive sensors to discriminate based on intensity modulation due to coning. The DITP 3D ladar not only has no problem in resolving such CSO's, it also has an inherent advantage in that the same amount of coning will result in 3 times as much modulation as the passive sensor would observe. Beyond that the 3D ladar can observe the actual variation in orientation once the targets are angularly resolved. This can cut through confusion the passive sensor could experience since different combinations of aspect and coning angle can yield the same modulation amplitude.

The ability of the 3D ladar to deliver such benefits hinged on the accuracy of its intensity measurements. Analysis backed by experiments indicates that while speckle is a potential problem, the intensity uncertainty it introduces can be mitigated by multi-pulse averaging. Sufficient engagement timeline exists for such an approach when proper-trades between pulse energy, rep rate, and beam profile are made. As evidenced by the ongoing demo flight integration effort this technology has advanced significantly beyond the laboratory demonstration stage. The integration effort surfaced many of the implementation issues, which in turn required a thorough understanding of speckle photon statistics.

4.0 ACKNOWLEDGEMENTS

This work was partially sponsored under BMDO/NRL contract N00014-97-D-2014 supporting the Discriminating Interceptor Technology Program. The authors would like to thank Dr. Frank Hanson, executing agent; LCDR James Buckley, program manager; and Dr. Walter Dyer, technical advisor, for their support and guidance. The authors wold also like to thank Guy Beaghler of Fibertek, Inc., and Dr. Daniel Leslie of ThermoTrex, Inc. for useful technical discussions concerning the DITP ladar system and photon statistics.

5.0 REFERENCES

1. Dyer, W., “Missile Seeker Technology at the Ballistic Missile Defense Organization,” Proc. AIAA Missile Sciences Conf., Dec. 1996.
2. Burnham, R., et al, “Short Pulse 3D Imaging Ladar for Advanced Target Discrimination,” Proc. IRIS Active Systems, Vol. 1, 1997.
3. Leslie, D., et al, “Direct Detection Laser Radar Angle/Angle/Range-Imaging Target Identification Capabilities,” Proc. IRIS Active Systems, Vol. 1, 1997.
4. Dyer, W., “Review of the Ballistic Missile Defense Organization’s Advanced Sensor and Seeker Technology Programs,” Proc. IRIS Active Systems, Vol., 1997.
5. Hart, G., et al., “Solid-state Laser Radar for DITP – New Discrimination Algorithms and Test Results with AMOR Targets,” Proc. IRIS Active Systems Conf. March 1998.
6. Hart, G., et al., “New Discrimination Algorithms and Test Results Using a Solid-state 3D Imaging Laser Radar,” Proc. 7th AIAA/BMDO Technology Readiness Conf., Aug. 1998.
7. MacFarland, A., et al., *Laser Cross Section Handbook*, Mission Research Corp., WRDC-TR-89-9010, June 1990.
8. Youmans, D, Hart, G., "Numerical evaluation of the "M" parameter for direct detection ladar," SPIE Proc. Vol. 3380, April 1998.
9. Yura, H., “Ladar detection statistics in the presence of pointing errors,” Appl. Opt., Vol. 33, No. 20, Sept. 1994.
10. Goodman, J., “Some Effects of Target-Induced Scintillation on Optical Radar Performance,” Proc. IEEE, Vol. 53, No. 11, Nov. 1965.
11. Goodman, J., “Comparative Performance of Optical-Radar Detection Techniques,” IEEE Trans. AES, Vol. AES-2, No. 5, Sept. 1966.
12. Goodman, J., *Laser Speckle and Related Phenomena*, J.C. Dainty Ed., Springer-Verlag, 1975, Second Edition, 1984.

13. Driscoll, T., et al., "Comparison of Theory and Experiments in the Effects of Speckle on NMD/TMD Target Recognition with Direct-Detection LADAR," Proc. IRIS Active Systems, Feb. 1999.

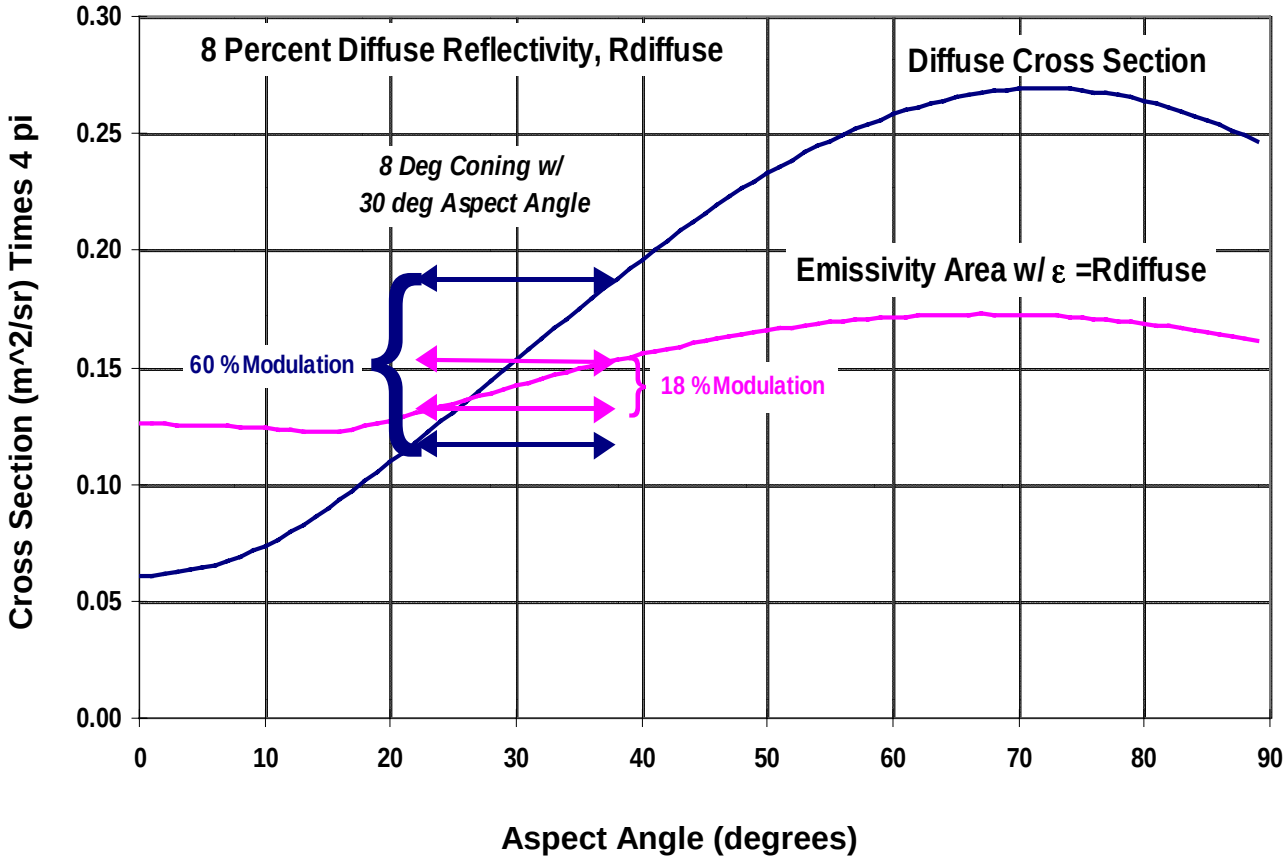

Figure 1. Cone (2m x 1m) LADAR Total Cross Section vs Aspect Angle

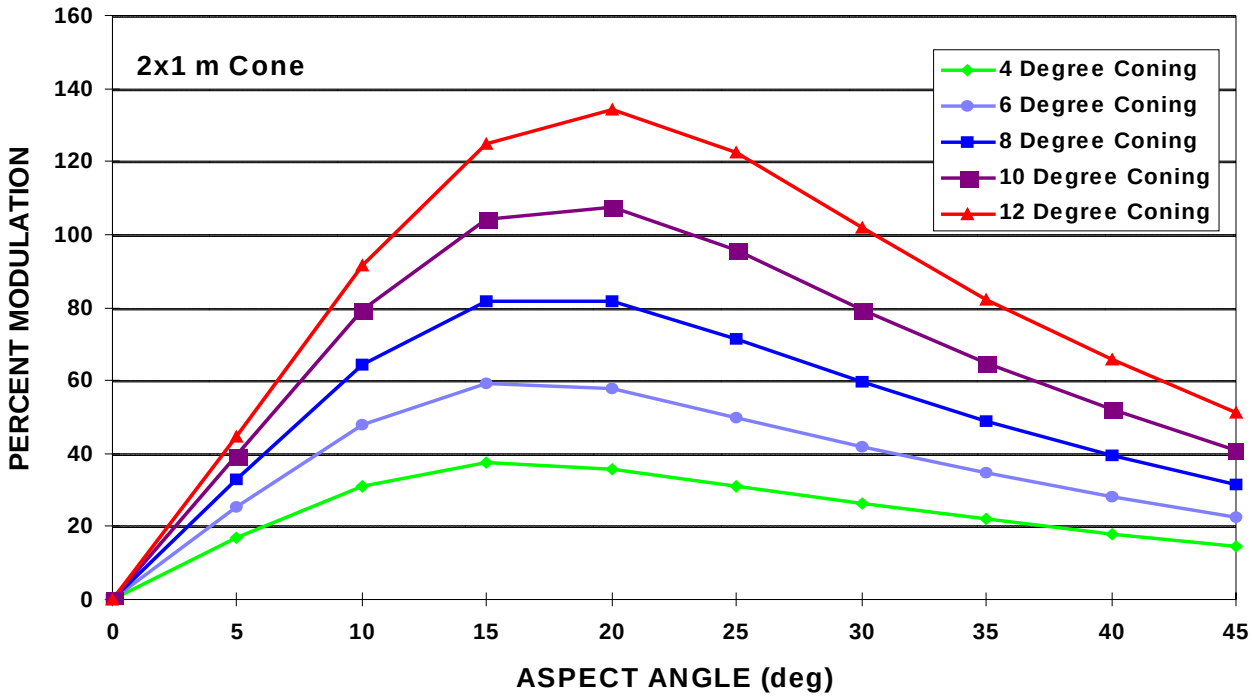

Figure 2. Intensity Modulation vs Aspect & Coning Angle

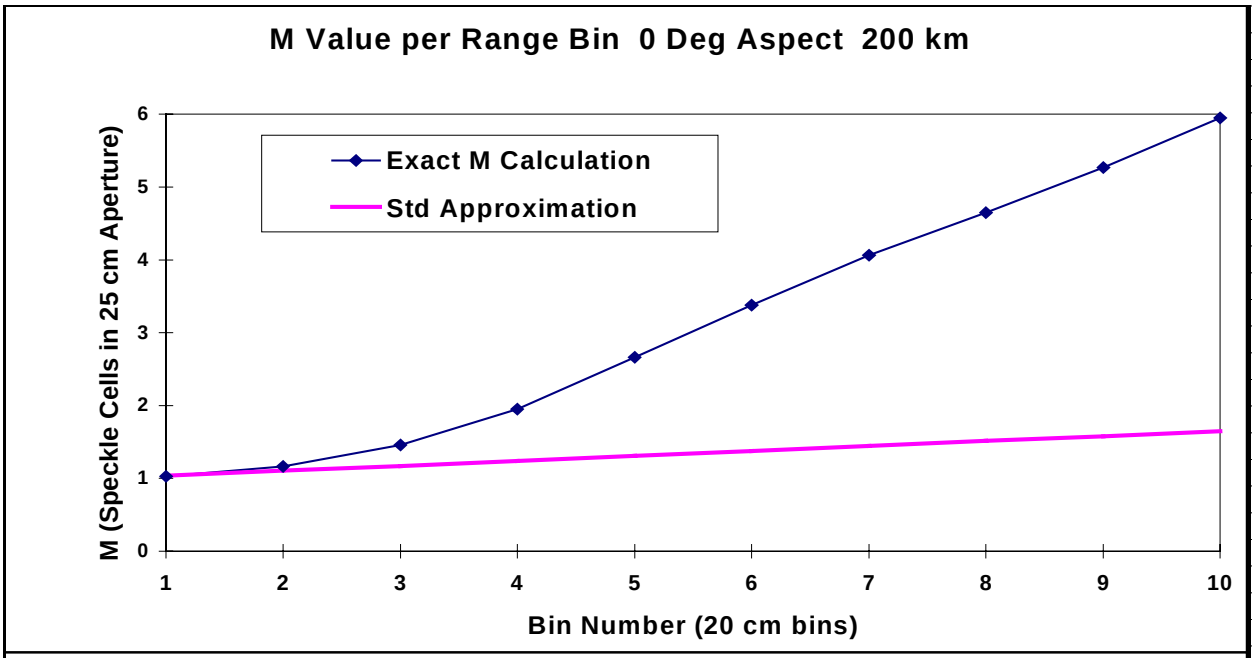

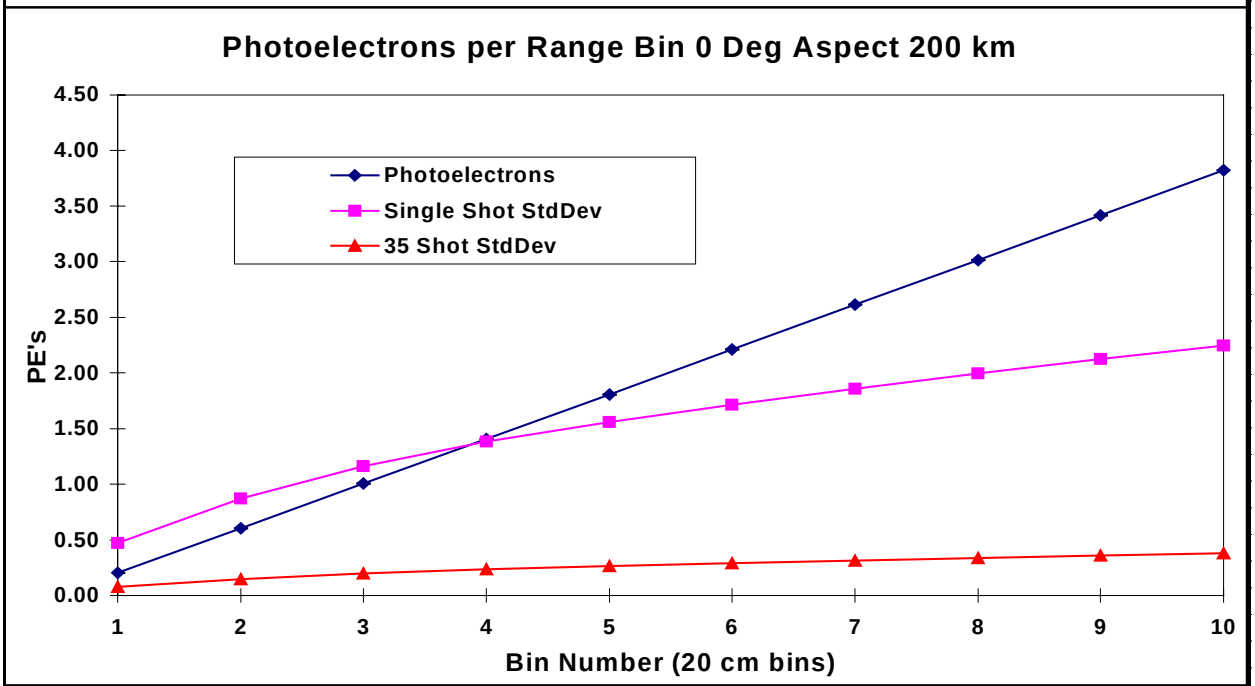

Range Bin	PE's	Weighting	Yura M	Yura Wgtd	Exact M	M weightd	Penalty	Sigma	35 Shot Si
1	0.20	0.05	1.03	0.05	1.03	0.05	5.459	0.470	0.079
2	0.60	0.16	1.10	0.17	1.16	0.18	2.089	0.872	0.147
3	1.01	0.26	1.17	0.31	1.46	0.38	1.337	1.162	0.196
4	1.41	0.37	1.24	0.46	1.95	0.72	0.967	1.384	0.234
5	1.81	0.47	1.31	0.62	2.66	1.26	0.741	1.557	0.263
6	2.21	0.58	1.37	0.80	3.38	1.96	0.600	1.713	0.290
7	2.61	0.68	1.44	0.99	4.06	2.78	0.506	1.859	0.314
8	3.02	0.79	1.51	1.19	4.65	3.67	0.439	1.998	0.338
9	3.42	0.89	1.58	1.41	5.27	4.72	0.387	2.128	0.360
10	3.82	1	1.65	1.65	5.95	5.95	0.346	2.246	0.380
Tot PE's	**20.11**			**7.65**	**<Mtarget>**	**21.67**	**0.073**		
				15.29	**Dual Polar**	**43.34**			

Figure 3. Speckle Analysis for 200 km Range 0 degree Aspect Angle

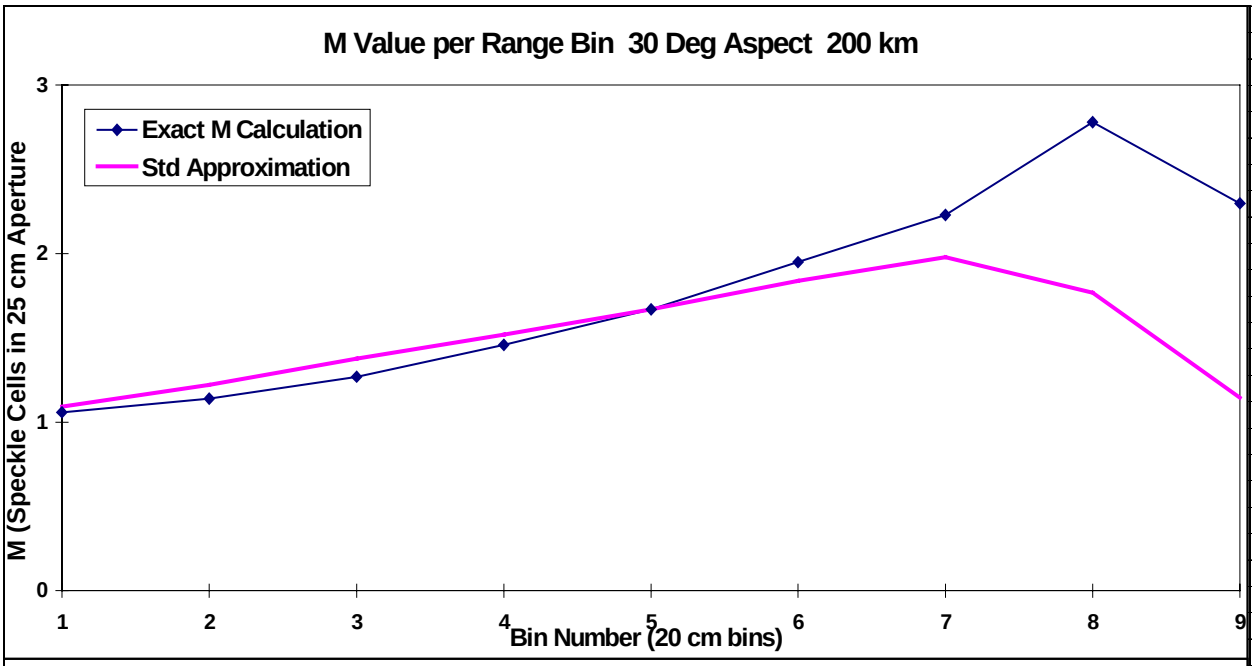

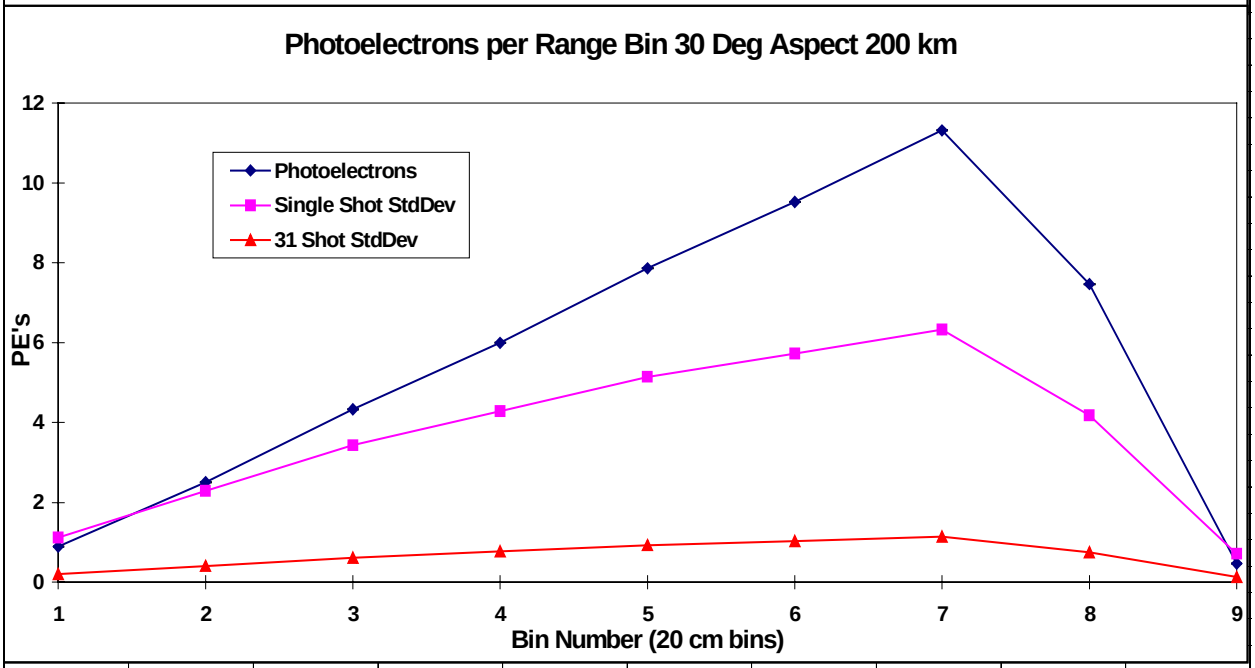

Range Bin	PE's	Weighting	Yura M	Yura Wgtd	Exact M	M weightd	(1/N+1/M)	Sigma	31 Shot Sig
1	0.88	0.08	1.09	0.09	1.06	0.08	1.602	1.120	0.201
2	2.50	0.22	1.22	0.27	1.14	0.25	0.838	2.291	0.411
3	4.33	0.38	1.38	0.53	1.27	0.49	0.625	3.424	0.615
4	6.00	0.53	1.52	0.81	1.46	0.77	0.509	4.280	0.769
5	7.87	0.69	1.67	1.16	1.67	1.16	0.427	5.137	0.923
6	9.52	0.84	1.84	1.55	1.95	1.64	0.361	5.723	1.028
7	11.32	1.00	1.98	1.98	2.23	2.23	0.313	6.328	1.137
8	7.47	0.66	1.77	1.17	2.78	1.83	0.314	4.183	0.751
9	0.46	0.04	1.15	0.05	2.30	0.09	2.374	0.714	0.128
10									
Tot PE's->	**50.35**			**7.59**	**<Mtarget>**	**8.55**	**0.078**		
				15.18	**Dual Polar**	**17.11**			

Figure 4. Speckle Analysis for 200 km Range 30 degree Aspect Angle

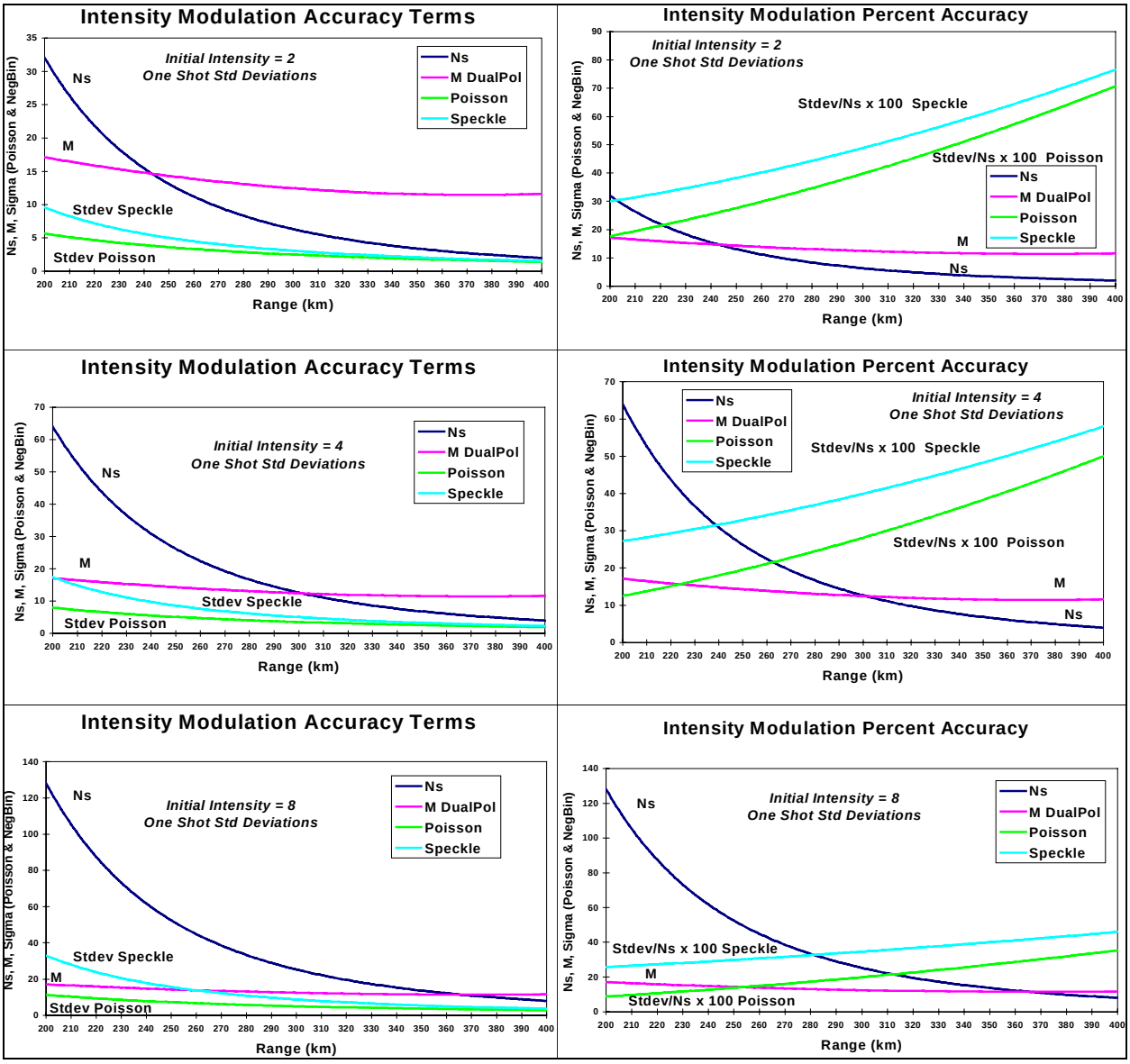

Figure 5. Speckle vs Range and Initial Intensity.

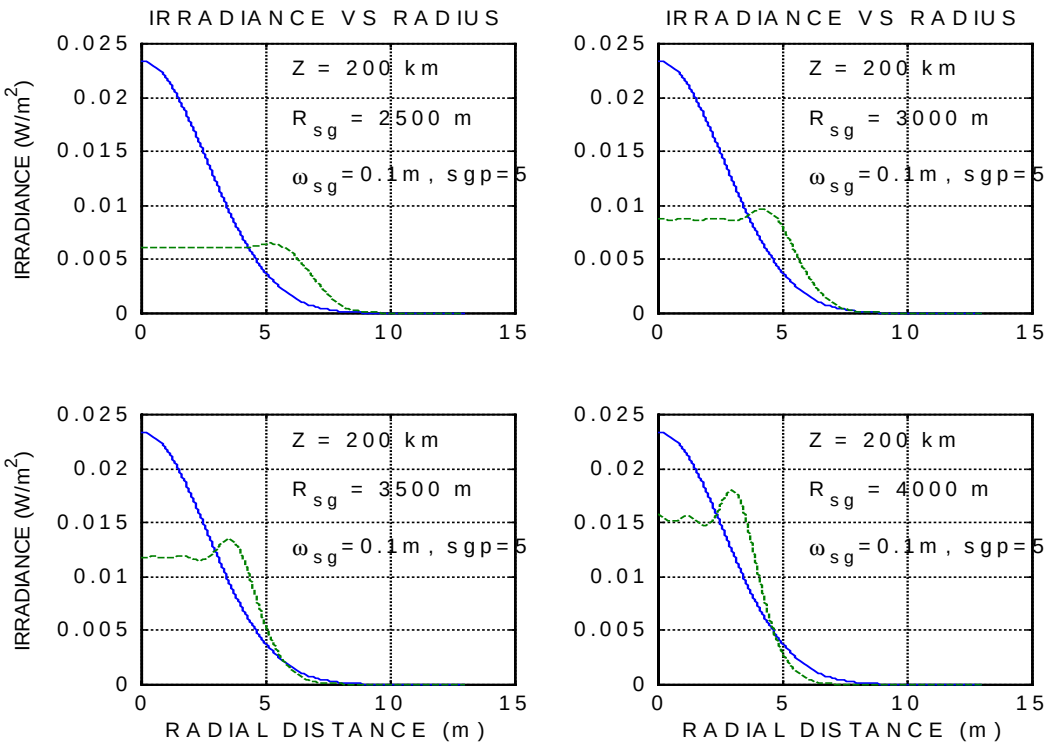

Figure 6. Irradiance (W/m^2) at 200 km range versus phase-front curvatures of 2500, 3000, 3500, and 4000 m. Solid line is reference Gaussian mode.

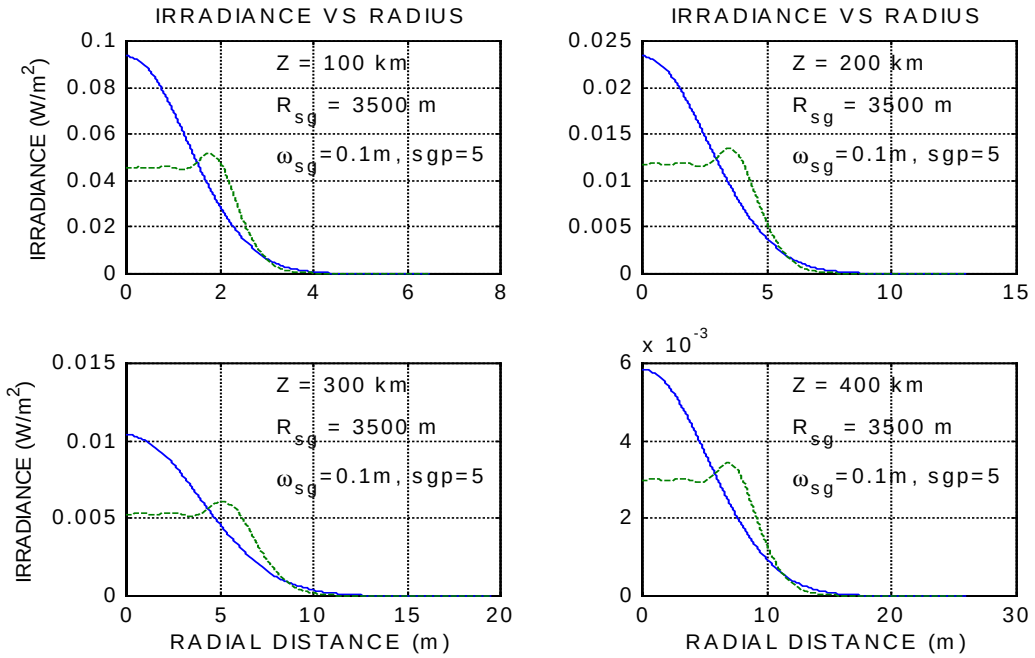

Figure 7. Irradiance (W/m^2) vs. radial distance at ranges of 100 km to 400 km with a constant phase front curvature of 3500 m. Solid line is reference Gaussian mode.